Gravitational waves in an interferometric detector

Archana Pai*

Indian Institute of Science Education and Research Thiruvananthapuram, CET Campus, Sreekaryam, Thiruvananthapuram 695 016, India

Detection of gravitational waves by two LIGO detectors has begun a new exciting era of gravitational wave astronomy. Following the two detections, India has stepped in the global effort towards gravitational wave observation via her involvement in the LIGO-India project. The LIGO-India project will open up new opportunities in the cutting edge and challenging field of gravitational wave detection. This article provides a background about gravitational waves and interferometric detector.

Keywords: Binary black holes, Fabry–Perot cavity, gravitational waves, interferometric detectors, LIGO detectors.

Introduction

THE historic announcement of observation of gravitational waves (GW) from binary black holes[1] on 11 February 2016 by LIGO Scientific Collaboration (LSC) and Virgo Collaboration was the first direct detection of GW (a century after its prediction in general relativity (GR)). The whole scientific community was excited with this discovery. GW event observed by the two LIGO (laser interferometric gravitational wave observatory) detectors located in Hanford and Louisiana, USA on 14 September 2015 (termed as GW150914) was a result of merger of two black holes (of masses 29 $M_\odot$ and 36 $M_\odot$ where $M_\odot$ is the solar mass), located at 1.33 billion light years (~410 Megaparsecs) (1 parsec (pc) = 3.26 light years = 2.06×10^5 Earth – Sun distance = 3.086×10^{16} m) away in a distant galaxy. In addition to being the first direct observation of GW, the event also provided first direct evidence of existence of black holes (BH) with masses >25 $M_\odot$ and first direct evidence of binary BH merger event. Following this, another binary BH merger event was observed on 26 December 2015 (termed as GW151226)[2] by the twin LIGOs and its detection was announced in June 2016 by the collaboration. The detection of two binary BH merger events from distant universe has opened up a new observational window – GW window to our universe. A new era of astronomy – GW astronomy – has begun with this landmark discovery and 2016 the special breakthrough prize in fundamental physics was announced for the detection of GW in May 2016 (ref. 3).

This article, we provide the basic physics concepts behind GW – sources and detectors, at the pedagogical level. It addresses the following topics – properties of GW, effect of GW on a collection of test masses, GW sources and optical laser interferometer as a GW detector. The article will also deal with the discovery of binary BH event in interferometric GW detector.

Gravitational waves in Einstein's gravity

In 1915, Einstein proposed the theory of gravity[4] i.e. general theory of relativity (GR). This theory revolutionized our view of the world as well as gave a new outlook to Newtonian picture of gravity. According to GR, all objects alter the space-time fabric around them and they move in this altered space-time fabric along the shortest path – geodesics. By the very nature, GR is intrinsically a non-linear theory. This is because any motion alters space-time fabric and this affects the motion of the object itself which in turn alters the fabric further and so on and so forth. To summarize, in GR, matter tells space how to curve, space tells matter how to move.

Till date, Einstein's GR is the most successful description of the world. In a weak gravity limit, GR approaches Newton's law of gravity. It could successfully explain all predictions of Newton's gravity such as planetary orbits, satellite motion, tides etc and could make new predictions. One of the greatest achievements of GR is the explanation of anomalous perihelion shift of Mercury's orbit. The perihelion of Mercury's orbit was showing an additional shift of 43 arc seconds per century. Newtonian gravity could not explain this shift successfully after incorporating effects of gravity due to other planets. However, within the framework of GR, motion of Mercury was successfully explained. Additional classical tests include bending of light, gravitational red-shift, gravitational lensing GW, etc. Most of the above predictions were tested with astronomical observations and GR passed with flying colours[5]. The only prediction which remained to be tested before GW150914, was the direct detection of GW. Now with the discovery of binary BH events, the last prediction of GR has been finally tested.

*e-mail: archana@iisertvm.ac.in

Gravitational waves

According to GR[6,7], GW are perturbations in space-time fabric that propagate away from the source with speed of light. In simple terms, they are like waves on the surface of water. For example, when we move a paddle in water, the water waves travel away from the paddle carrying information about motion of the paddle. Similarly orbital motion of Earth around Sun is like paddling in space. This motion produces GW and carries away energy/momentum from the source with speed of light.

These perturbations are produced due to non-zero non-spherical acceleration of objects. An example of non-zero non-spherical accelerating motion in day-to-day life could be spinning objects, merry-go-round, smashing objects, orbiting planets, earthquakes, etc. A large variety of objects around us are continuously emitting GW – quite similar to accelerating charges around us are continuously emitting electromagnetic (EM) waves e.g. radio, mobile phones, microwave oven, light bulb, TV towers, people, etc.

Consider a collection of charged particles oscillating with frequency ω confined in a region of radius R. According to classical electrodynamics, the accelerating charges emit EM waves far away from the source *aka* in far zone. The far zone condition is

$$\text{Distance } r \gg \text{wavelength } \lambda >> \text{source size } R, \tag{1}$$

where $\lambda \equiv 2\pi c/\omega$ is the wavelength of EM waves emitted due to oscillating charges. The above condition culminates into two conditions:

(a) *Far field:* Distance to the source is much greater than the source size (R) and thus the EM field is not dominated by Columbian field (i.e. not $1/r^2$ terms as they die down much rapidly).
(b) *Slow motion:* The velocity of oscillating charges is low. Therefore EM waves travel much faster than the variation of oscillating charge within the source. This condition translates into $R \ll \lambda$.

Thus, under slow motion case, information of the oscillating motion of charges is carried away by EM waves travelling away from the source in far field. EM waves also carry energy and momentum along with them.

Now, let us consider an oscillating gravitating source with frequency ω and confined in the region of radius R. We ask an analogous question: What is the nature of waves produced by an accelerating gravitating source? Again there are two conditions: (1) gives weak gravity, i.e. the distance is much larger than the source size. Therefore, perturbation produced is on the flat (Minkowskian) space-time; slow motion condition (2) ensures that information travels much faster than the variation of source density.

Under the above two conditions, Einstein's GR predicts radiative solution in terms of GW. Emitted GW carry away information of the intrinsic motion of the source[4]. The amplitude of GW is expressed in terms of a second-rank tensor known as GW tensor; h_{ij} and is written as

$$h_{ij}(t) \sim \frac{2G}{rc^4}\ddot{I}_{ij}(t - r/c), \tag{2}$$

where $\ddot{I} = d^2I/dt^2$. Mass quadrupole moment tensor at time t

$$I_{ij}(t) = \int \rho(\mathbf{x}, t)\left(x_i x_j - \frac{1}{3}\delta_{ij}x^2\right)\mathrm{d}^3x, \tag{3}$$

is defined for continuous mass distribution of density $\rho(\mathbf{x}, t)$. The indices i, j correspond to spatial coordinates along the direction perpendicular to GW propagation. This tensor is symmetric in nature, i.e. $h_{ij} = h_{ji}$. For example, if GW is propagating along z-direction with respect to the observer, then x_1 and x_2 are x and y-components of $\mathbf{x}$. Therefore, non-zero h_{ij} would be h_{xx}, h_{xy}, h_{yy}. Rigorous derivation of this formula can be found in ref. 8. This tensor can be treated as a small perturbation to the background at (Minkowskian) space-time. Mass quadrupole moment is a measure of anisotropy of mass distribution. Any spherically symmetric accelerated motion produces zero quadrupole moment and thus will not emit GW. Therefore, GW measures the non-spherical kinetic energy of the source at a given time instance. GW amplitude decreases inversely with distance – property of a wave.

Below we compare the properties of GW with that of EM waves.

- EM waves are produced due to oscillating charges. GW are produced due to nonspherical accelerated motion of objects.
- GW are quadrupolar in nature whereas EM waves are dipolar in nature[9].
- EM waves include varying electric and magnetic fields which are vectorial quantities. GW h_{ij} is perturbation to the flat space-time fabric which is a tensor quantity.
- Both EM waves and GW are transverse in nature. i.e. fields oscillate perpendicular to the direction of propagation of waves.
- EM wave travels with the speed of light in vacuum or free space. In Einstein's GR, GW travels with the speed of light.
- GW window probes macroscopic dynamics of the gravitating system. EM waves probe microscopic oscillation of charges in the system. This clearly shows that EM and GW observation of same source can provide a completely complementary picture of the given source. Thus, EM and GW window together can shed more light on the underlying physics of the source.

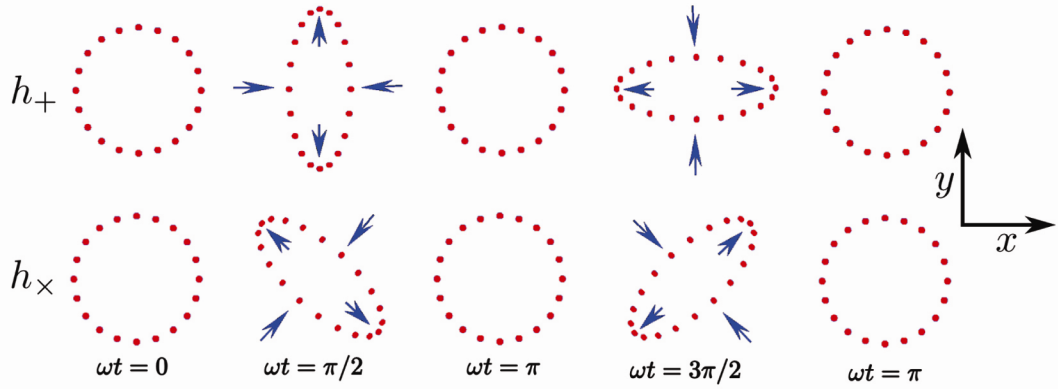

Figure 1. Effect on a ring of particles with respect to time if GW is incident perpendicular to the plane of paper. h_+ and $h_\times$ denote GW polarizations. (Figure credit: K. Haris).

Effect of incoming gravitational wave on test masses

To detect GW, it is crucial to understand the effect of incident GW on test masses. Consider an incoming GW in z-direction; according to GR, they produce strain in the plane perpendicular to the direction of propagation, i.e. strain is produced in x–y plane. Since what one measures is the change in length, a minimum of two test masses separated in space are necessary to study the effect of GW. Here, what we mean by test masses are objects free from any other force. They only experience effects of incoming GW.

In Einstein's GR, GW carry two polarizations h_+ ($h_{xy} = 0$) and $h_\times$ ($h_{xx} = 0 = h_{yy}$). Consider a ring of test particles as shown in Figure 1 in a circle (with $\omega t = 0$ case). If (+) polarized GW is incident from z-direction (along the direction perpendicular to the plane of the paper), the ring will get elongated and contracted during the two half cycles of GW as shown by the first row in Figure 1. If (×) polarized GW is incident, the ring will show deformations as shown by the second row of Figure 1. The terminology '+' and '×' pertains to the pattern of primary axes along which this deformation takes place. In general, GW will be a combination of both polarizations.

A typical strain produced in separation of size L is of the order h. Thus, passing GW produces changes in length of the order of hL. Clearly, longer the separation between two test masses, higher would be the change which can be detected. Further, stronger the source (higher GW amplitude), larger will be the strain produced.

Observation of an astrophysical GW source in a given detector depends on various factors – first and foremost is to check if the source is emitting GW in that frequency band. If yes, then the next thing to check is whether the band-passed accumulated signal power in that frequency band is sufficiently higher than the noise level. The third deciding factor is whether we can claim an observation with a certain level of confidence. In the rest of the article, we discuss some of these factors. The first factor depends on the nature of GW source and strength of GW it emits. Below, we give the order of magnitude estimates and typical signal strengths. The second factor depends on GW frequency emitted by known sources and the response of the detector at those frequencies. These points are addressed in the later section. The third factor crucially depends on the noise characteristic of the detector. We do not discuss this factor in this article. Interested readers can look at ref. 8 for details.

Estimate of gravitational wave strength

While GR predicted GW in 1916, it took almost a century to directly detect them. Direct observation of GW remained a challenging problem partly due to tiny strains produced by GW sources. In other words, the space-time fabric is a stiff fabric. Enormous energy is needed to produce tiny perturbations on it.

To understand this, we make order of magnitude estimates of strength (amplitude) of GW. Let us drop indices in eq. (4) and represent quadrupole moment term by $\ddot{I} \sim M v^2_{N\mathrm{Sph}}$. This is termed as non-spherical part of kinetic energy. Non-spherical means not distributed spherically. For a gravitating system, we write $v^2 = -(GM/R)$. If we replace $v^2_{N\mathrm{Sph}}$ by GM/R, we get an upper bound on $\ddot{I}$ (bound because only non-spherical part of v^2 contributes to GW and not the whole). Therefore, we obtain an upper bound on the amplitude of GW as a product of dimensionless internal energy and external energy of the system[10] and is given below

$$h < \frac{2GM}{Rc^2}\frac{GM}{rc^2} \sim \alpha \Phi_{\mathrm{ext}}. \tag{4}$$

The quantity $\alpha \equiv 2GM/Rc^2$ is known as compactness parameter. This parameter quantifies how compactly the object of mass M is packed in radius R. Classically, α is also the ratio of squares of escape velocity (velocity required to escape from the surface of that object. For Earth, the escape velocity is 11 km per second) and the

velocity of light c (300,000 km per second). Since no physical entity can travel greater than the speed of light, the maximum value of α is unity. Closer the α approaches unity, more compact is the object, higher is the gravity and hence higher is the curvature of space-time around that system. For a single BH, $\alpha = 1$, i.e. BH are objects with escape velocity equal to speed of light. For neutron stars (NS) (neutron stars are end stages of stellar evolution of stars with mass > 6 $M_\odot$. They are primarily made up of neutrons with mass of 1.4 $M_\odot$ and radius of 10 km), $\alpha = 0.4$. For our sun $\alpha = 4 \times 10^{-6}$. Our Sun is million times less compact than the BH.

Equation (4) clearly shows that the amplitude of GW is a small fraction (given by α) of dimensionless Newtonian potential. This implies that the strength of GW is, in general, small compared to Newtonian potential and compact objects emit strong GW. GW frequency of any GW source is twice its dynamical frequency. The dynamics can be of any nature such as orbital, rotational, precessional, etc. Amplitude of few known GW sources is estimated below:

- *A spinning rod on Moon:* Consider a spinning rod of mass, M of 1 kg; length, L of 1 metre and spinning at frequency, f of 10 cycles per seconds located, on Moon. The spinning rod produces time varying quadrupole moment – $v_{NSph}/c \sim L\omega/c \sim 2 \times 10^{-7}$. Distance to the moon from Earth (Earth-moon distance is one light second) is 20 times the GW wavelength. Therefore, for a detector on Earth the GW amplitude from this spinning rod is $h < 10^{-49}$. This will produce an equivalent strain on Earth. However, strains of such order cannot be measured with current technology.
- *Earth–Sun system:* Consider the gravitationally bound Earth–Sun system. As Earth orbits around the Sun, the system radiates GW. Let us assume the observer is located at 1 kpc. It is easy to check that it satisfies far-zone condition. We estimate GW amplitude as

$$h < 10^{-8}\left(\frac{GM_\odot}{Rc^2}\right)^2 < 10^{-24}, \tag{5}$$

  This is much higher than the spinning rod.
- *Binary system with two stars:* Consider a binary system with two compact stars and total mass M, orbital separation R located at distance r. The upper bound on GW amplitude can be obtained based on eq. (4) as

$$h \le 5 \times 10^{-23}\left[\frac{M}{2.8M_\odot}\right]^2\left[\frac{R}{200\text{ km}}\right]^{-1}\left[\frac{r}{100Mpc}\right]^{-1}, \tag{6}$$

  The typical estimate of GW amplitude for NS binary system located at 100 Mpc separated by orbital separation of 200 km, is 5×10^{-23}. The two stars approach each other as they evolve, making the system more and more compact and emit GW with higher and higher amplitude. Presently, there are 13 binary pulsars (rotating NS) with NS companions which are observed in EM window. We choose typical numbers of NS binary for binary scaling relation.

Thus, from the above three examples, it is evident that besides distance, compactness parameter also plays a crucial role in determining the GW strength. Higher the compactness parameter, higher is GW amplitude. A large variety of astrophysical sources involve compact objects. Prominent candidates include binary systems with BH and/or NS, Pulsars (with asymmetrical shape), core collapse supernova (end stages of massive star >10 $M_\odot$ undergoing aspherical core collapse), merging galaxies (super massive BH (SMBH) mergers at centres of the galaxies) and accreting systems (BH accreting mass from a massive star).

Gravitational wave frequency band

GW frequency crucially depends on the dynamics of the system. A large variety of GW objects involve binary systems with compact objects such as NS–NS, NS–BH, BH–BH, SMBH–SMBH. Observation of such objects in GW window can unearth a wealth of physics which has not been probed by EM window. For example, we have not observed NS–BH system in EM window yet and the binary BH merger events was the first ever BH merger event observed by LIGO detectors.

In this section, we estimate the frequency band of GW. Here we compute the typical frequency emitted by binary system during its inspiral evolution. Consider a binary system of total mass M and orbital separation R. When the two stars are well separated, they can be treated as point masses and orbital motion is governed by Kepler's third Law of Planetary Motion $\omega^2 R^3$ = constant with ω as the angular frequency. Instantaneous GW frequency emitted by such a system is twice its orbital frequency. The scaling relation is given by

$$f_{GW} \sim 64\text{ Hz}\left[\frac{M}{2.8M_\odot}\right]^{1/2}\left[\frac{R}{200\text{ km}}\right]^{-3/2}. \tag{7}$$

Thus, the GW frequency of NS–NS binary system separated by 200 km is ~64 Hz. As the two stars orbit, the system loses energy in the form of GW. The orbital radius decreases and hence orbital frequency increases following Kepler's law. Thus, in this evolutionary phase, GW frequency increases with respect to time, known as inspiral phase. It is clear that from eq. (7), the frequency of GW emitted by NS–NS for separation of 200,000 km is 2 mHz. The same source emits GW frequency spanning four orders of magnitude. Therefore, when the stars are

farther away, GW strength will also be smaller as the system is less compact. On the other hand, two SMBH at centres of galaxies can emit GW from nanoHz to mHz. Thus, binary systems can span several orders of magnitude in GW.

Complex systems such as supernova explosion need detailed numerical simulation to arrive at waveform models[11]. The frequency emitted from such systems can range from few tens of Hz to hundreds of Hz. Further, isolated pulsars can emit GW up to kHz (pulsars with millisecond period have been observed in EM band).

GW spectrum can span several orders of magnitude right from nanoHz to kHz based on total masses and evolutionary phase of the astrophysical system under consideration. A large variety of GW projects ranging from pulsar timing arrays (PTA)[12], future space-based detector (laser interferometric space antenna (LISA)[13]) and ground based laser interferometric detectors can cover a large fraction of GW window.

EM window spans 16 orders of magnitude from radio waves (10 kHz) to gamma rays (10^{19} Hz). Observations of an astrophysical object in different windows probe different physical and dynamical features of the same object. Likewise, different GW detectors, space as well as ground based detectors, will probe different frequency band complementary to each other as well as to the EM window. This will probe various dynamical aspects of the same object and help in reconstruction of properties of the object in GW band.

Laser interferometric gravitational wave detector

The two LIGO detectors located in USA are 4 km arm-length, suspended Michelson type laser interferometers with Fabry–Perot cavities. They are sensitive to broad band frequency between 20 Hz and 1 kHz. LIGO frequency band spans the audio frequency band and hence GW observations is referred as Listening to GW from the Universe. In this section, we briefly explain the main factors which allow a Michelson interferometer to act as a GW detector.

As explained earlier, the incoming GW alter space-time fabric. When the distance between two test masses is much smaller than the wavelength of GW, GW produces strain in the distance of order of amplitude of GW (h). In the previous section, we estimated typical GW amplitude from different terrestrial as well as astrophysical sources. Typical GW amplitude from an astrophysical source is 10^{-21}–10^{-23}. The detector needs to have very high sensitivity to detect such small strains. Strain of the order of 10^{-21} corresponds to a change in the radius of the Earth by an amount as small as the size of an atomic nucleus. Hence, because of such small numbers, detection of GW was a huge challenge for almost a century after its prediction. Thanks to the advancement of laser technology in 1980s with subsequent improved techniques in precision measurement, that LIGO detector is a reality today with this magnificent discovery of GW[14].

Principle of Michelson interferometer

In a simple Michelson interferometer, a laser beam is split into two beams by a beam splitter and sent to two orthogonal directions towards two-end mirrors. The beams get reflected from the mirrors back to the beam-splitter. At the beam-splitter, the two beams interfere and part of them is sent to the output photodiode. Photodiode converts the incident photons into photo current. If the arms are of same length (or multiple of laser wavelength λ_l), destructive interference is produced and no light enters the photodiode. All the light goes back to the laser. If this condition is not satisfied then the light photons will enter photodiode. Photodiode converts the incident light into an equivalent photo current and voltage which is measured at the output.

If L_1 and L_2 are lengths of the two arms then the optical path difference is equal to the difference in their length. The corresponding phase difference is $2\pi/\lambda_l$ times the path difference. Light beams interfere destructively when the phase difference is odd multiple of π. This is the basic principle of Michelson interferometer. If the optical path length changes then some additional light gets recorded. See for details ref. 15.

Michelson interferometer as a GW detector

Consider a GW incident on the interferometric detector with wavelength λ. If $\Delta L \ll \lambda$, then the strain produced in arm 1 due to incoming GW is given by $\Delta L_1 \sim hL_1$ and similar for arm 2. Michelson interferometer measures this change in length as $\Delta L \equiv \Delta L_1 - \Delta L_2$. The corresponding phase difference is computed. The performance of Michelson interferometer as a GW detector crucially depends on its ability to measure minute phase difference produced by an incoming GW.

Let us consider that we want to measure $h \sim 10^{-21}$. Now the question is to bring together all different ideas needed to achieve this seemingly impossible task. If we assume that a simple Michelson is sensitive to changes in length equal to the wavelength of laser λ_l, then with Nd-Yag laser (1.064 micrometer wavelength) and LIGO-like (4 km) arm-length, the corresponding strain would be

$$h \sim \lambda_l/L \sim 10^{-10}. \quad (8)$$

This is 11 orders of magnitude higher than the target sensitivity to be achieved. Following is partial list of ideas that have been adopted to achieve this sensitivity[8] (Figure 2).

- Fabry–Perot cavities: Effective increase in Michelson's arm-length. The physical length of the detector is

restrictive and cannot be increased beyond few km. Curvature of the Earth starts becoming prominent with increase in L. For example, for 4 km arm-length, Earth's curvature displaces laser beam vertically by one metre[16]. An alternative and effective technique of increasing arm-length is to introduce Fabry–Perot optical cavity in each arm. This is termed as light storage arm in Figure 2.

Fabry–Perot cavity consists of two mirrors forming an optical cavity. When light enters this cavity, it makes several round trips before it exits the cavity. The finesse of cavity (an optical parameter which depends on the reectivity of two mirrors) is directly proportional to an average number of round trips of light inside the cavity. The effective length of Michelson interferometer with Fabry–Perot cavity is then $L_{\text{eff}} \sim L\mathcal{F}/(2\pi)$; for details see ref. (15)). Addition of cavities improves h given in eq. (8) by at least maximum 2 orders of magnitude.

- Increased laser power: Improved photon shot noise. The ability to measure small changes in light intensity depends on the efficiency of the photodiode. Photodiode is limited by photon counting noise termed as the photon shot noise. The rate at which photons arrive at photodiode in a given time interval follows Poisson's statistics. Thus, if the number of photons arrived in the time interval T is N, the corresponding variation in N is $\sqrt{N}$. This variation limits the performance of photodiode. The photon shot noise at photodiode becomes $\Delta\phi_{\text{Ph}} = N^{-1/2}$. If the accumulated phase due to GW is greater than this noise $\Delta\phi_{\text{Ph}}$, then the apparatus becomes sensitive to GW. GW phase will be

$$\Delta\phi_{\text{GW}} = \frac{2\pi}{\lambda_l} L_{\text{eff}} h. \tag{9}$$

For $h \sim 10^{-21}$ and $L_{\text{eff}} \sim 500$ km and $\Delta\phi_{\text{GW}} \sim 3 \times 10^{-9}$. This implies that the number of photons required is $N \sim 10^{17}$. For T ~ 1.6 msec, the condition $\Delta\phi_{\text{GW}} > \Delta\phi_{\text{Ph}}$ requires a laser power of 12 watts. By increasing laser power, one can combat the photon shot noise and achieve the desired sensitivity. However, with increase in power, photons gain sufficient energy to push mirrors and mimic the effect of GW. This is called radiation pressure noise. A balance needs to be achieved between the photon shot noise and radiation pressure noise.

- Suspended optics: Improves the seismic noise. Increasing laser power improves the high frequency response. However, at low frequencies (few tens of Hz), seismic motions (motion of the floor at low frequency due to human activity as well as other seismic activity) alter the interferometer's position mimicking the incident GW. This is one of the prime noise sources at low frequencies. Multiple stage suspensions are used to reduce the low frequency noise. Typically the pendulum response goes as $(1/f^2)^k$ above resonant frequency with k being the number of suspension levels[18].

In addition to the main ideas for improvement listed above, the whole apparatus needs to be kept in ultra-high vaccum. An extensive list of noise sources and corresponding techniques to circumvent are listed in ref. 17. Details regarding the advanced LIGO detector are available in refs 16–19. To summarize, the detector noise curve can be described by shape of a bucket with the floor at around 120 Hz (best sensitivity) and gradually increasing with frequency on both sides of 120 Hz. Therefore, the typical frequency band of interferometric detector like LIGO ranges between 20 Hz and about 1 kHz. Noise below the frequency of 20 Hz and above 1 kHz is very high and the interferometer is blind outside the bucket.

Current global advanced interferometric GW detector network includes twin LIGOs of 4 km arm-length located at Hanford and Louisiana, USA, the French-Italian Virgo located at Pisa[20,21] of 3 km arm-length, the Japanese KAGRA detector at Kamioka site with arm-length of 3 km (refs 22, 23) and the LIGO India (USA – Indian GW interferometric detector of arm-length 4 km to be commissioned in India)[24].

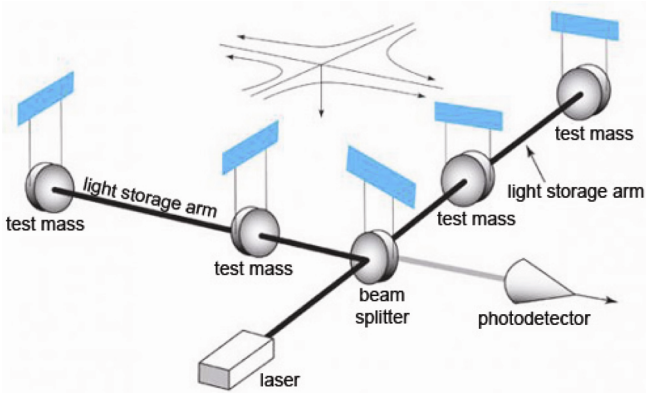

Figure 2. Suspended Michelson interferometer with Fabry–Perot cavities acts as a GW detector. (Credit: LIGO.)

Compact binaries in interferometric detectors

Compact binaries are prime target sources of interferometric detectors. Compact binary evolution goes through three phases; inspiral, merger and ringdown. In inspiral phase, two stars slowly approach each other through successive binary orbits which are smaller and smaller in size. As they approach each other, they orbit with higher and higher velocities and hence emit binary chirp waveform with increasing frequencies as a function of time. GW emitted from binary during this inspiral phase is called binary chirp – a frequency modulated signal[11]. Further, the rate of increase in frequency in inspiral phase is higher at high frequencies as well as for massive objects. Thus, the same binary system would emit monochromatic GW if observed much earlier in time (at lower

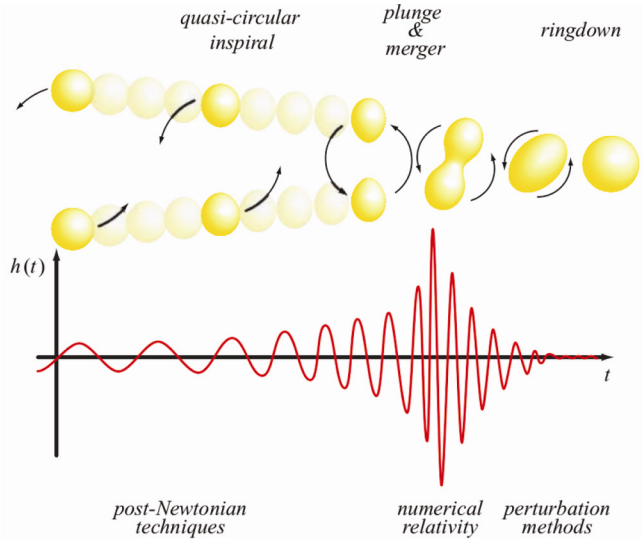

Figure 3. A schematic of binary evolution through inspiral, merger and ringdown phases (Credit: ref. 29).

frequency). In merger phase, two stars come close to each other and finally merge. In ringdown phase, the final star (most likely a BH) slowly settles down to its quiescent state as a damped sinusoid (Figure 3).

The interferometer starts observing GW from an astrophysical binary when its frequency is above the lower frequency of the band f_s (e.g. 20 Hz). For example, for NS binary system (following eq. (7)), GW frequency becomes 20 Hz when the distance between the two objects becomes ~420 km.

The duration of different phases depends on the masses of the two objects. For example, higher the masses, faster is the inspiral phase and shorter will be its duration. More specifically, duration of the inspiral phase is governed by chirp mass $\mathcal{M} = \mu^{3/5}M^{2/5}$ which is the combination of reduced mass $\mu = M_1M_2/M$ and total mass M of the system. Inspiral duration is

$$\tau \sim 260\left(\frac{\mathcal{M}}{30M_\odot}\right)^{-5/3}\left(\frac{f_s}{30\text{ Hz}}\right)^{-8/3}\text{ m sec}, \quad (10)$$

Thus, for equal mass ratio system $\mu = 0.25M$ and τ varies as $M^{-5/3}$. Inspiral duration for binary BH of 30–30 $M_\odot$ system is 400 msecs as opposed to 23 sec for binary NS when f_s is 30 Hz. With improved seismic noise, the lower frequency of the detector band further lowers down. For a low frequency limit of 20 Hz, the chirp duration further increases by $(3/2)^{8/3}$. The subsequent merger phase lasts for a very small fraction of msecs. The ringdown frequency (f_{RD}) for the dominant mode as well as damping time depends on total mass of the binary as

$$f_{RD} \sim 260\left(\frac{65M_\odot}{M}\right)\text{Hz}, \quad (11)$$

and damping time

$$\tau_{RD} \sim 4\left(\frac{M}{65M_\odot}\right)\text{m sec}. \quad (12)$$

The first GW event detected by twin LIGO (GW150914) lasted for ~200 msecs between 35 and 250 Hz (ref. 1) in LIGO band with peak GW strain of $\sim 10^{-21}$. The masses of the individual binary stars were estimated to be 29 $M_\odot$ and 36 $M_\odot$ respectively. Using eq. (10), one can obtain the duration of the inspiral phase. The final BH mass was estimated to be 62 $M_\odot$. Therefore, the system was estimated to emit energy in GW equivalent to 3 $M_\odot$. The merger event GW150914, arrived at LIGO-Livingston 7 msec before LIGO-Hanford. Due to proximity of the two LIGO detectors, the source was poorly localized in the southern sky within ~600 sq. deg. (The full moon subtends 0.2 sq. deg. in the sky.) The open data for the two GW events is available at LIGO Open Science Center[25]. In ref. 26, the basic physics of GW150914 event is discussed.

Era of GW astronomy

A new era of GW astronomy has begun with the discovery of two BH binary merger event. With more and more data pouring in from currently operating LIGOs, we expect to observe more events of binary BHs[27]. In addition to binary BHs, detection of binaries with NS will shed light on the structure of NS – one of the open questions in NS star physics. In the coming decade, more detectors will join the two advanced LIGOs, such as advanced Virgo, KAGRA and LIGO-India. With this addition, we improve sky coverage (large part of the sky is visible), observe much deeper in the universe and understand the source better[28], with better estimation of binary parameters (distance, source inclination as well as direction). Due to the unique location of LIGO-India, i.e. the light travel time between LIGO-Livingston and India being close to 39 msec (maximum amongst the detector pairs), the interferometric detector network can localize GW source by two orders of magnitude after LIGO-India joins the network. Increase in GW detections from compact binaries, will reveal the distribution of compact binaries as well as BHs in our universe. Till date, no direct observation of NS–BH binaries has been made in EM band. Observation of NS–BH binaries in GW window will tell us more about binaries and their formation story.

In addition to ground-based interferometers, space-based LISA will observe in low frequency bands up to 1 Hz. Together with LISA and LIGO-like interferometers, GW window will span 8 orders of magnitude in frequency band[11]. We expect the universe to unfold many more surprises to us.

1. Abbott, B. P. *et al*., Observation of gravitational waves from a binary black hole merger. *Phys. Rev. Lett*., 2016, **116**, 061102-2–061102-16.
2. Abbott, B. P. *et al*., (LIGO scientific and Virgo Collaborations) GW151226: Observation of gravitational waves from a 22-solar-mass binary black hole coalescence. *Phys. Rev. Lett*., 2016, **116**, 241103-1–241103-14.
3. https://breakthroughprize.org/News/32
4. Schutz, B. F., *A First Course in General Relativity*, Cambridge University Press, Cambridge, UK, 1985.
5. Will, C. M., *Theory and Experiments in Gravitational Physics*, Cambridge University Press, Cambridge, UK, 1981.
6. Einstein, A., *Approximative Integration of the Field Equations of Gravitation*, Sitzungsber. K. Preuss. Akad. Wiss., 1, 1916, pp. 688–696.
7. Einstein, A., *Über Gravitationswellen*, Sitzungsber. K. Preuss. Akad. Wiss., 1, 1918, pp. 154–157.
8. Creighton, J. and Andersson, W., In *Gravitational-wave Physics and Astronomy*, Wiley Series in Cosmology, Wiley-VCH Verlag GmbH, KGaA, Germany, 2011.
9. Thorne Kip, S., Multipole expansions of gravitational radiation. *Rev. Mod. Phys*., 1980, **52**, 299–339.
10. Schutz, B. F., Gravitational waves on the back of an envelope. *Am. J. Phys*., 1984, **52**, 412–419.
11. Sathyaprakash, B. F. and Schutz, B. F., Physics, astrophysics and cosmology with gravitational waves. *Living Rev. Relativity*, 2009, **12**(2), 1–141.
12. http://www.ipta4gw.org/
13. https://www.elisascience.org/
14. Drever, R., Raab, F., Thorne, K., Vogt, R. and Weiss, R., In Laser Interferometer Gravitational-wave Observatory (LIGO) Technical Report, 1989; https://dcc.ligo.org/LIGOM890001/public/main
15. Hecht, E., *Optics*, Addison Wesley, May 1987, 2nd edn.
16. https://www.ligo.caltech.edu/page/facts
17. Adhikari, R., Gravitational radiation detection with laser interferometry. *Rev. Mod. Phys*., 2014, **86**, 121–151.
18. Saulson, P., *Fundamentals of Interferometric Gravitational Wave Detectors*, World Scientific, 1994.
19. Abbott, B. P. *et al*. (LIGO Scientific and Virgo Collaborations) GW150914: The advanced LIGO detectors in the era of first discoveries. *Phys. Rev. Lett*., 2016, **116**, 131103-1–131103-12 (preprint 1602.03838).
20. Brillet, A. *et al*., Virgo Project Technical Report No. VIR-0517A-15, 1989; https://tds.egogw.it/ql/?c=11247
21. The Virgo Collaboration 2012 Advanced Virgo Technical Design Report Tech. Rep. VIR-0128A-12 Virgo Collaboration.
22. Aso, Y. *et al*., The KAGRA collaboration. Interferometer design of the KAGRA gravitational wave detector. *Phys. Rev*., 2013, **D88**(4), 043007-1–043007-15 (preprint 1306.6747).
23. Somiya, K., Detector configuration of KAGRA – the Japanese cryogenic gravitational-wave detector. *Class. Quant. Grav*., 2012, **29**, 124007 (preprint 1111.7185).
24. Ligo-India, Proposal of the Consortium for Indian Initiative in gravitational-wave observations (indigo). Tech. Rep. LIGO-M1100296-v2, 2011.
25. LIGO Open Science Center; https://losc.ligo.org/about/
26. Abbott, B. P. *et al.* (LIGO Scientific and Virgo Collaborations), The rate of binary black hole mergers inferred from advanced LIGO observations surrounding GW150914. *ApJL*, 2016, **833**, L1 (preprint 1602.03842).
27. Abbott, B. P. *et al.* (LIGO Scientific and Virgo Collaborations), The basic physics of the binary black hole merger GW150914, *Ann. Phys*., 2017, **529**(1–2), 1600209 (preprint 1608.01940).
28. Tagoshi, H., Mishra, C., Pai, A. and Arun, K. G., Parameter estimation of neutron star-black hole binaries using an advanced gravitational-wave detector network: Effects of the full post-Newtonian waveform. *Phys. Rev. D*, 2014, **90**, 024053.
29. Baumgarte, Thomas, W. and Shapiro Stuart, L., *Numerical Relativity*, Cambridge University Press, Cambridge, UK, 2010.

ACKNOWLEDGEMENTS. This document has LIGO-Document No: P1600356. I thank Ofek Birnholtz and Chandra Kant Mishra for useful comments.

doi: 10.18520/cs/v112/i07/1353-1360